Mon. Not. R. Astron. Soc. **425,** 1951–1957 (2012) doi:10.1111/j.1365-2966.2012.21483.x

Noise bias in weak lensing shape measurements

Alexandre Refregier,[1⋆] Tomasz Kacprzak,[2] Adam Amara,[1] Sarah Bridle[2] and Barnaby Rowe[2,3,4]

[1]*Institute for Astronomy, ETH Zurich, Wolfgang-Pauli-Strasse 27, CH-8093 Zurich, Switzerland*
[2]*Department of Physics & Astronomy, University College London, Gower Street, London WC1E 6BT*
[3]*Jet Propulsion Laboratory, California Institute of Techonology, 4800 Oak Grove Drive, Pasadena, CA 91109, USA*
[4]*California Institute of Technology, 1200 East California Boulevard, Pasadena, CA 91106, USA*

Accepted 2012 June 8. Received 2012 May 29; in original form 2012 March 22

ABSTRACT

Weak lensing experiments are a powerful probe into cosmology through their measurement of the mass distribution of the universe. A challenge for this technique is to control systematic errors that occur when measuring the shapes of distant galaxies. In this paper, we investigate noise bias, a systematic error that arises from second-order noise terms in the shape measurement process. We first derive analytical expressions for the bias of general maximum-likelihood estimators in the presence of additive noise. We then find analytical expressions for a simplified toy model in which galaxies are modelled and fitted with a Gaussian with its size as a single free parameter. Even for this very simple case we find a significant effect. We also extend our analysis to a more realistic six-parameter elliptical Gaussian model. We find that the noise bias is generically of the order of the inverse-squared signal-to-noise ratio (SNR) of the galaxies and is thus of the order of a percent for galaxies of SNR 10, i.e. comparable to the weak lensing shear signal. This is nearly two orders of magnitude greater than the systematic requirements for future all-sky weak lensing surveys. We discuss possible ways to circumvent this effect, including a calibration method using simulations discussed in an associated paper.

Key words: gravitational lensing: weak – methods: statistical – techniques: image processing – cosmology: observations – dark energy – dark matter.

1 INTRODUCTION

Weak gravitational lensing is a technique to map the distribution of dark matter in the universe (see e.g. Refregier 2003; Hoekstra & Jain 2008, for reviews). It relies on the measurement of the apparent shapes of distant galaxies that are distorted due to matter inhomogeneities along the line of sight. Weak lensing offers great prospects for the measurement of cosmological parameters (Albrecht et al. 2006; Peacock & Schneider 2006). In particular, the measurements of dark energy parameters with future wide-field surveys are very promising but place strong requirements on weak lensing measurements and in particular in the control of systematics.

The main potential systematic effects are generally considered to be (i) galaxy shape measurement from galaxy images, (ii) galaxy distance measurement using photometric redshifts, (iii) galaxy intrinsic alignments arising from the galaxy formation process and (iv) the accuracy of theoretical predictions of dark matter clustering. We focus on the first of these in this paper.

In most cases, the gravitational lensing effect produces matrix distortion stretching of the galaxy image. This image shear must be uncovered in the presence of nuisance observational effects, including image blurring due to the atmosphere and telescope optics, image pixelization due to the nature of photon detectors and noise due to the finite number of photons from the galaxy and other backgrounds. Furthermore, the intrinsic properties of the galaxy prior to lensing distortion are unknown.

The first detection of this shearing effect was made by Tyson, Wenk & Valdes (1990) and repeated by Bonnet, Mellier & Fort (1994) who also developed methods for removing the image convolution effects. This was taken to a new level by Kaiser, Squires & Broadhurst (1995) in a method that is widely referred to as KSB and that has remained the most widely used shear measurement method to this day. Essentially, the KSB method uses weighted quadrupole moments of images to calculate shears and corrects the shears for the weight function. This was further improved in Kaiser (2000). An alternative approach using a simple galaxy model to forward fit the data was proposed in Kuijken (1999), and implemented in Bridle et al. (2002) and Miller et al. (2007). More flexible models using Gauss–Laguerre polynomials, or shapelets, have also been proposed (Bernstein & Jarvis 2002; Refregier & Bacon 2003). Each of these

⋆E-mail: alexandre.refregier@phys.ethz.ch

approaches has potential strengths and drawbacks. For instance, the limitations of model-fitting methods were explored in Melchior et al. (2010) and Voigt & Bridle (2010), and potentially mitigated by Bernstein (2010).

There have been several simulation challenges to assess how well current methods can measure gravitational shear and to encourage the development of new methods. The Shear TEsting Programme (STEP) 1 Challenge provided a suite of simulated images using relatively simple galaxy models but a realistic image blurring model. The galaxies were distributed with random positions across the image, and the same shear was used to distort every galaxy in a given large image. It was found that the existing methods that had already been applied to observational data were sufficiently good to merit the science results on those data (Heymans et al. 2006).

The STEP2 Challenge used more realistic galaxy models and a wider range of blurring models (Massey et al. 2007), and reached similar conclusions despite this additional complexity. However, neither challenge was sufficiently large to forecast the efficacy of existing methods for use on future surveys, and neither challenge was able to address *all* potential sources of measurement bias in real data (such as uncertainty about the image point spread function or PSF; see e.g. Paulin-Henriksson et al. 2008; Paulin-Henriksson, Refregier & Amara 2009; Rowe 2010). In addition, while it was possible in many cases to positively detect biases in weak lensing shape measurement methods, due to the complexity and realism of the STEP challenges it was not always possible to attribute definite causes for these effects. In the complex, multistage analysis required for weak lensing measurement, it can be very difficult to isolate individual causes of systematic bias, and yet diagnosing these individual contributions is an important ongoing process in the development of an accurate measurement methodology.

The GRavitational lEnsing Accuracy Testing 2008 (GREAT08) Challenge was much simpler: it reverted to simpler galaxy models, avoided overlapping galaxies and used similar properties for all galaxies in a large image (Bridle et al. 2009). It was designed to attract new methods from outside the weak lensing community, in particular from computer scientists. Most significantly, the number of galaxies was chosen to test methods at the level required for surveys in the foreseeable future, as calculated in Amara & Réfrégier (2007). A new approach won the competition, inspired by Kuijken (1999), which took the advantage of the fact that the same shear was used for many galaxies at a time, by 'stacking' the galaxies (Hosseini & Bethge 2009; Lewis 2009). Although progress has been substantial, questions still remain about the likely issues that need to be overcome to reach the precision needed for future all-sky surveys.

In this paper, we study noise bias, one of the systematic effects that can affect weak lensing measurements. It arises from high-order noise terms in the measurement of the shape parameters of galaxies, increasing in magnitude at a low galaxy signal-to-noise ratio (SNR). Its effects on second-order moment measurements from convolved Gaussian galaxy images have been described by Hirata et al. (2004).

To study this effect in the context of forward-fitting weak lensing measurement, we first derive general expressions for the variance and bias of maximum-likelihood estimators (MLEs) of model parameters in the presence of additive Gaussian noise (Section 2). We then apply them to a one-parameter toy model consisting of the maximum-likelihood (ML) fitting of the size of a Gaussian galaxy model to a Gaussian galaxy convolved with a known Gaussian PSF (Section 3). While this model is clearly oversimplified, it illustrates the principle of noise bias and its amplitude. We then extend this result by considering a more realistic model consisting of an elliptical Gaussian galaxy with six free parameters (Section 4). In Section 5, we discuss the consequences of our findings and possible remedies, and summarize our conclusions, including a calibration method using simulations discussed in an associated paper (Kacprzak et al. 2012, hereafter K12).

2 GENERAL 2D SHAPE ESTIMATION

In this section, we study the general problem of the estimation of the shape parameters of a 2D object in the presence of additive, uncorrelated Gaussian noise. For weak lensing, these results are applicable to the measurement of galaxy shapes and to the estimation of the instrument PSF using stars in the image. The general analytical results that we derive will serve as a useful base for comparison with the more realistic conditions studied by K12 using numerical simulations.

2.1 General results

Let us thus consider the observed 2D surface brightness $f_{\rm obs}(\boldsymbol{x})$ of an object that is described by a model $f(\boldsymbol{x};\boldsymbol{a})$, where $\boldsymbol{x}$ is the position on the image and $\boldsymbol{a}$ is the vector of parameters describing the shape of the object. We can write the observed surface brightness as

$$f_{\rm obs}(\boldsymbol{x}) = f(\boldsymbol{x};\boldsymbol{a}^{\rm t}) + n(\boldsymbol{x}), \tag{1}$$

where $\boldsymbol{a}^{\rm t}$ are the true shape parameters of the object and $n(\boldsymbol{x})$ is the noise which is assumed to be uncorrelated and Gaussian with $\langle n(\boldsymbol{x})\rangle = 0$ and $\langle n(\boldsymbol{x})^2\rangle = \sigma_{\rm n}^2$.

With these assumptions, the log likelihood of the data given the model is $\ln L = -\chi^2/2$, where the usual χ^2 function is given by

$$\chi^2(\boldsymbol{a}) = \sum_p \sigma_{\rm n}^{-2}\left[f_{\rm obs}(\boldsymbol{x}_p) - f(\boldsymbol{x}_p;\boldsymbol{a})\right]^2, \tag{2}$$

where the sum is over all pixels p in the image.

The MLE $\hat{\boldsymbol{a}}$ for the shape parameters of the object can then be constructed by requiring that χ^2 is minimized at $\boldsymbol{a} = \hat{\boldsymbol{a}}$. MLEs were first studied by Fisher (1922), and then later by Rao (1973) and Cramér (1999). They are commonly used estimators in statistics and have several desirable properties, including consistency that requires that in the limit of high SNR the MLE recovers the true values $\boldsymbol{a}^{\rm t}$ of the estimated parameters.

In Appendix A, we derive general properties for the MLE $\hat{\boldsymbol{a}}$ using an expansion in the inverse SNR of the object. There and in what follows, we label SNR using the parameter ρ. We first show that the covariance of the estimated parameters is, to leading order, given by

$$\mathrm{cov}[\hat{a}_i, \hat{a}_j] = (F^{-1})_{ij} + O(\rho^{-4}), \tag{3}$$

where the Fisher matrix is given by

$$F_{ij} = \sum_p \sigma_{\rm n}^{-2}\frac{\partial f(\boldsymbol{x}_p;\boldsymbol{a}^{\rm t})}{\partial a_i}\frac{\partial f(\boldsymbol{x}_p;\boldsymbol{a}^{\rm t})}{\partial a_j}. \tag{4}$$

We also find that the bias in the parameters $b[\hat{a}_i] = \langle\hat{a}_i\rangle - a_i^{\rm t}$ is given by

$$b[\hat{a}_i] = -\frac{1}{2}(F^{-1})_{ij}(F^{-1})_{kl}B_{jkl} + O(\rho^{-4}), \tag{5}$$

where the summation convention over repeated indices is assumed and the bias tensor is given by

$$B_{ijk} = \sum_p \sigma_{\rm n}^{-2}\frac{\partial f(\boldsymbol{x}_p;\boldsymbol{a}^{\rm t})}{\partial a_i}\frac{\partial^2 f(\boldsymbol{x}_p;\boldsymbol{a}^{\rm t})}{\partial a_j\partial a_k}. \tag{6}$$

It is often useful to consider functions $g_i(\boldsymbol{a})$ of the parameters. The covariances of these functions are given by

$$\mathrm{cov}[g_i, g_j] = \frac{\partial g_i}{\partial a_k}\frac{\partial g_j}{\partial a_l}\mathrm{cov}[a_k, a_l], \tag{7}$$

while their bias is given by

$$b[g_i] = \frac{\partial g_i}{\partial a_k} b[a_k]. \tag{8}$$

2.2 Properties

As can be seen from equation (5), the bias tensor depends on second-order derivatives of the model $f(\boldsymbol{x}, \boldsymbol{a})$ in the parameters $\boldsymbol{a}$ and therefore vanishes for linear models. This restates the known fact that MLEs may be biased in general, except in the case of linear models. As noted in Appendix A, the present bias arises from second-order noise terms and is therefore referred to as 'noise bias'.

We then note that the squared error in the parameters $\sigma^2[a_i] = \mathrm{cov}[a_i, a_i]$ and the bias $b[a_i]$ are of the order of

$$b[\hat{a}_i]/a_i^{\mathrm{t}} \sim [\sigma[\hat{a}_i]/a_i^{\mathrm{t}}]^2 \sim \rho^{-2}, \tag{9}$$

in dimensionless units. In the limit of high SNR, $\rho \to \infty$, both tend to zero so that the estimator tends to the true value $\hat{\boldsymbol{a}} \to \boldsymbol{a}^{\mathrm{t}}$, thus recovering the consistency property of MLEs (e.g. Cramér 1999).

For finite values of ρ, the statistical error and bias of the parameters can be non-negligible. Weak lensing shape measurements are typically performed down to $\rho \sim 10$ to maximize the surface density of galaxies. In this case, the statistical rms error will be of the order of $\rho^{-1} \sim 0.1$ which is consistent with the typical observed shape noise per galaxy of about $\delta\gamma \sim 0.3$, and which includes this statistical measurement error and the distribution of the intrinsic shape of galaxies. The bias in the parameters in this regime will be of the order of $\rho^{-2} \sim 0.01$ which is comparable to the weak lensing shear signal $\gamma \sim 0.02$ and may contribute to explain why some methods do not perform better (e.g. Bridle et al. 2009). As shown by Amara & Réfrégier (2007), the requirement for the variance of the shear systematics is $\sigma^2_{\mathrm{sys}} \sim 10^{-7}$ which corresponds to the systematic shear error of $\delta\gamma \sim 3 \times 10^{-4}$. This is almost two orders of magnitude smaller than that predicted by the current analysis of noise bias.

We also note that the expressions for the variance and bias of the MLEs are expressed in equations (3) and (5) in terms of a sum over pixel positions, but can often be more conveniently evaluated in the continuum limit where the pixel size is small compared to the object size. This approximation is given by equation (A8), re-expressing the sum as an integral over the 2D image. In Section 3.3, we show that this approximation holds for moderate pixel sampling of the object. However, we expect that the undersampling arising from the finite pixel size present in practice will tend to increase the amplitude of the bias.

Seemingly counter-intuitively, the bias of the derived parameters $g_i(\hat{\boldsymbol{a}})$ is not equal in general to the bias that would be derived had it instead been chosen to find the MLE of the parameters $\hat{g}_i$ directly. This can be understood from examining the covariance transformation rule described in equation (7). Thus, the exact value of the bias for any parameter of interest may depend on the parametrization of the model itself. We will show an example of this property in the following simplified example.

3 CIRCULAR GAUSSIAN MODEL

To illustrate the above results, we first consider the case of the measurement of the size of a 2D, circular, Gaussian galaxy without any other free parameters. This is a highly simplified illustration of the shape measurement problem and should therefore be considered as a toy model that captures the main features of the effect of noise bias.

3.1 Case without PSF convolution

First, let us consider the case where the galaxy is not convolved with the PSF of the instrument. In this case, the galaxy surface brightness is given by

$$f(\boldsymbol{x}; a) = f_0 \exp\left[-\frac{r^2}{2a^2}\right], \tag{10}$$

where $r^2 = x_1^2 + x_2^2$, f_0 is a normalization controlling the flux of the galaxy and a is the rms size.

To characterize the SNR ρ of the galaxy, we temporarily consider f_0 as the free parameter while keeping a fixed. Using the continuum limit (equation A8), we can analytically integrate equation (3) for the variance of the estimator for f_0 and obtain

$$\rho[f_0] = \frac{f_0}{\sigma[f_0]} = \frac{\sqrt{\pi} f_0 a}{\sigma_{\mathrm{n}} h}, \tag{11}$$

where h is the pixel scale and σ_{n} is the noise rms as in Section 2. Here and in the following, we drop the $\hat{}$ and $^{\mathrm{t}}$ symbols to simplify the notation when it does not lead to ambiguities. This definition of the SNR can be considered as the ideal detection SNR of the galaxy, corresponding to perfect knowledge of the galaxy shape and position, or equivalently to an ideal matched filter.

Now, considering a as the only free parameter (and thus leaving f_0 fixed), we again integrate equation (3) analytically in the continuum limit and obtain

$$\frac{\sigma[a]}{a} = \frac{1}{\sqrt{2}}\rho[f_0]^{-1} + O(\rho^{-2}), \tag{12}$$

which scales as ρ^{-1}, as noted in Section 2.2. Integrating equation (5), we find that the bias in this case vanishes at second order, i.e. $b[a] = 0 + O(\rho^{-4})$. This is due to a cancellation which, we find, occurs for any 2D circular galaxy model which can be written as

$$f(\boldsymbol{x}; a) = f_0 \phi(r/a), \tag{13}$$

where ϕ is any function describing the galaxy profile. Interestingly, this cancellation only occurs in two dimensions, and the second-order bias term does not vanish in one or more than two dimensions even if the above scaling symmetry holds.

3.2 Case with PSF convolution

Let us now consider the case of interest in practice where the circular Gaussian galaxy is convolved with a PSF due to the instrument and the atmosphere. In the spirit of the toy model, we make the simplifying assumption that the PSF is itself circular and Gaussian with an rms size q. Since the convolution of two Gaussians is another Gaussian with standard deviations adding in quadrature, the model in this case is

$$f(\boldsymbol{x}; a) = f_0 \exp\left[-\frac{r^2}{2(a^2 + q^2)}\right], \tag{14}$$

where f_0 is a normalization controlling the flux of the galaxy. The PSF size q is assumed to be known and the noise is assumed to be Gaussian with an rms of σ_{n}.

In this case, the ideal SNR defined as in Section 3.1 becomes

$$\rho = \frac{f_0}{\sigma[f_0]} = \frac{\sqrt{\pi} f_0 \sqrt{a^2+q^2}}{\sigma_n h}, \tag{15}$$

and the uncertainty in the MLE for a is given by

$$\frac{\sigma[a]}{a} = \frac{1}{\sqrt{2}} \left[1 + \left(\frac{q}{a}\right)^2\right] \rho[f_0]^{-1} + O(\rho^{-2}). \tag{16}$$

Because the presence of the PSF breaks the scaling symmetry of equation (13), the bias does not vanish to second order, and we find

$$\frac{b[a]}{a} = -\frac{1}{4} \left[1 + \left(\frac{q}{a}\right)^2\right] \left(\frac{q}{a}\right)^2 \rho[f_0]^{-2} + O(\rho^{-4}). \tag{17}$$

We note that we recover the results of Section 3.1 without a PSF when we set $q = 0$ in the expressions above. We also note that the scalings of equation (9) hold for the rms error and bias with pre-factors that depend on the ratio of the galaxy to PSF size.

We also note that if we had instead estimated the convolved galaxy parameters directly and obtained the deconvolved size as a derived parameter (using equation 8), the bias would then have vanished to this order. But this would also allow unphysical values of the parameters, with $a^2 < 0$. This is an illustration of the fact that the bias of physical parameters depends in general on the specific parametrization of the estimated model, as discussed in Section 2.2.

3.3 Simulations

In order to check the validity of the expansion described in Section 2 and Appendix A, and gain insights into the origin of the bias, we performed numerical simulations of this toy model. We considered a range of SNR for a circular Gaussian galaxy of true size $a^t = 4$ convolved with a circular Gaussian PSF of size $q = 5.33$ pixels. This corresponds to a ratio of the convolved galaxy size to the PSF size of $\sqrt{a^{t2}+q^2}/q \simeq 1.25$ which is typically used as the limit for weak lensing surveys.

Even for this simple one-parameter toy model, we find that care must be taken for the implementation of the minimization of the χ^2 function. Readily available minimizers appeared to lead sometimes to sensitivity to internal parameters and artefacts at the level of precision required for weak lensing. For the present simulation, we instead computed $\chi^2(a)$ on a grid in the interval $0.1 < a < 10$ pixels with a grid size of $\Delta a = 0.0033$ pixels and found the minimum by direct search.

Fig. 1 shows the resulting probability distribution function (PDF) $P(a)$ of the estimator for a for a range of SNR $\rho[f_0]$. At high SNR, the PDF is nearly Gaussian and peaks close to the true value $a^t = 4$ pixels. As the SNR decreases, the PDF's main peak shifts towards the right, while a secondary peak at $a = 0$ starts developing. The complicated combination of these two effects contributes to the dependence of the bias and rms error on SNR.

Fig. 2 shows the dependence of the rms variance $\sigma[a]$ on the SNR $\rho[f_0]$. We see that our expression in equation (3) is a good approximation for $\rho[f_0] \gtrsim 10$. The deviations below this value are not surprising since higher order terms are expected to become important in the low SNR limit.

Fig. 3 shows the dependence of the bias $b[a]$ on the SNR $\rho[f_0]$. Again, our expression in equation (5) is a good approximation for SNR $\gtrsim 10$, with deviations below this value likely due to higher order terms. The horizontal dashed line in the lower panel corresponds to the requirement for future all-sky surveys $b[a]/a \simeq \delta\gamma \simeq 3 \times 10^{-4}$, as discussed in Section 2.2 and in Amara & Réfrégier (2007). The bias for galaxies with SNR ~ 10 in this toy model is $b[a]/a \simeq 0.015$, which is nearly two orders of magnitude greater than this requirement and comparable to the expected weak lensing signal $\delta\gamma \simeq 0.02$.

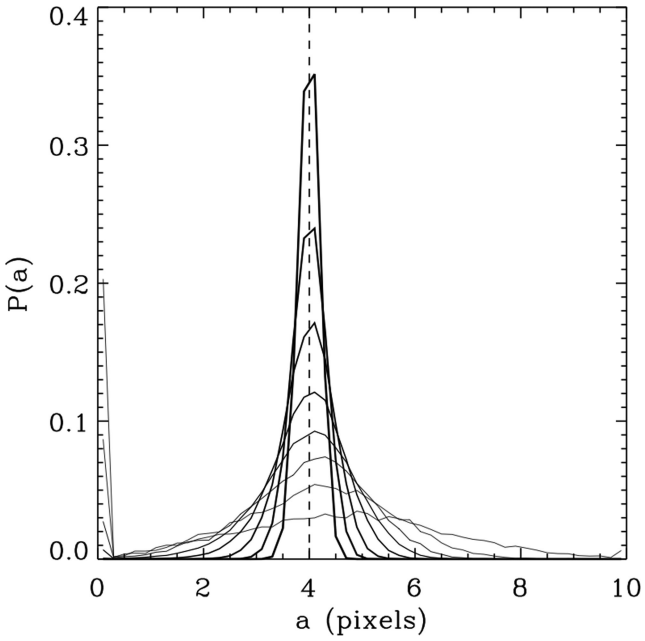

Figure 1. Distribution $P(a)$ of the MLE for the size a of the 2D Gaussian from repeated realizations. The curves from broad (thin lines) to sharp (thick lines) correspond to the SNR $\rho[f_0]$ of 3, 5, 7, 9, 12, 17, 25, 40, respectively. The true value of the parameter $a^t = 4$ pixels is shown as the vertical dashed line. The PSF size is $q = 5.33$ pixels corresponding to a ratio of the convolved galaxy size to the PSF size of $\sqrt{a^{t2}+q^2}/q \simeq 1.25$.

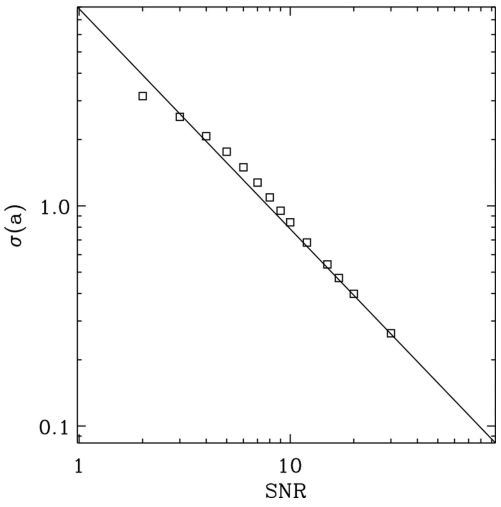

Figure 2. Standard deviation $\sigma[a]$ of the size estimator a as a function of SNR $= \rho[f_0]$. The expectation from the analytical prediction (solid line) is compared to the measurements from repeated experiments.

4 ELLIPTICAL GAUSSIAN MODEL

We now consider a slightly more realistic model of a galaxy consisting of a 2D elliptical Gaussian galaxy with six parameters. This is the smallest number of parameters needed to measure galaxy shapes for weak lensing in practice as they correspond to the two centroid coordinates, flux, major and minor axes and position angle of the galaxy. In practice, the models for galaxies are typically

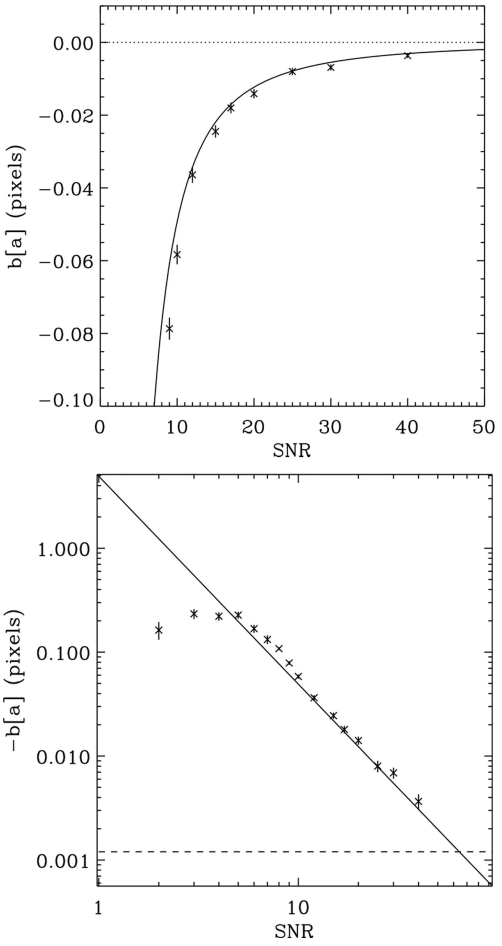

Figure 3. Bias $b[a]$ of the size estimator a as a function of SNR $= \rho[f_0]$ in linear (upper panel) and log (lower panel) axes. In both panels, the solid line corresponds to the analytical model, while the squares were derived from simulations of repeated experiments. The horizontal dashed line in the bottom panel corresponds to the requirement for future all-sky surveys (see the text).

non-Gaussian and more complicated in order to better describe realistic galaxies. The six-parameter Gaussian model is nevertheless useful to study the behaviour of the bias in the multiparameter case.

Let us thus consider a galaxy surface brightness given by a 2D elliptical Gaussian (without PSF convolution) that we parametrize as (see also Paulin-Henriksson et al. 2008 for a slightly different parametrization)

$$f(\boldsymbol{x};\boldsymbol{a}) = \frac{f_0}{2\pi\sqrt{a_1 a_2}} \exp\left[-\frac{1}{2}(\boldsymbol{x}-\boldsymbol{x}^a)^{\mathrm{T}}\mathbf{A}^{-1}(\boldsymbol{x}-\boldsymbol{x}^a)\right], \tag{18}$$

where a_1 and a_2 are the (rms) major and minor axes of the Gaussian, respectively, f_0 is a parameter which determines the amplitude, $\boldsymbol{x}^a$ is the centroid and superscript T denotes the transpose operator. The quadrupole moment matrix $\mathbf{A}$ is a 2×2 symmetric matrix which can be written as

$$\mathbf{A} = \mathbf{R}(\alpha)^{\mathrm{T}} \begin{pmatrix} a_1^2 & 0 \\ 0 & a_2^2 \end{pmatrix} \mathbf{R}(\alpha), \tag{19}$$

where α is the position angle of the major axis counter-clockwise from the x-axis and

$$\mathbf{R}(\alpha) = \begin{pmatrix} \cos\alpha & \sin\alpha \\ -\sin\alpha & \cos\alpha \end{pmatrix} \tag{20}$$

is the rotation matrix which aligns the coordinate system with the major axis. In Appendix B, we show that the amplitude, centroid and quadrupole moment matrix are simply related to the multipole moments of galaxy surface brightness.

Let us consider the MLEs for this 2D Gaussian with the following six free parameters:

$$\boldsymbol{a} = \left(x_1^a, x_2^a, f_0, a_1, a_2, \alpha\right). \tag{21}$$

In the continuum limit (equation A8), the Fisher matrix equations (4) can be computed analytically. This is facilitated by rotating into the coordinate system aligned with the major and minor axes of the galaxy before performing the integral of the surface of the galaxy. The resulting Fisher matrix F_{ij} and covariance matrix $\mathrm{cov}[a_i, a_i]$ of the parameters are given in equation (B4) in Appendix B. We note that, with this parametrization, the Fisher matrix is conveniently nearly diagonal.[1] The corresponding rms statistical errors $\sigma[a_i] = \mathrm{cov}[a_i, a_i]^{1/2}$ are listed in the third column in the top part of Table 1, to leading order in the SNR of the amplitude f_0 defined as

$$\rho[f_0] \equiv \frac{f_0}{\sigma[f_0]} = \frac{f_0}{\sqrt{4\pi}h\sigma_{\mathrm{n}}}. \tag{22}$$

Using equation (5) after the same change of coordinates and some cumbersome algebra, we can also derive the bias in the model parameters which are given in equation (B5) and listed in the last column of Table 1. Note that several of the parameters have a singularity as the galaxy becomes circular, i.e. when $\epsilon = 0$, which occurs at $a_1 = a_2$. This follows from the fact that, in this limit, the position angle α becomes degenerate.

From these expressions and using equations (7) and (8), we can derive the error and bias for derived quantities. The lower part of Table 1 provides the definition, statistical errors and biases for several commonly used parameters such as the flux $F^{(0)}$ (see also equation B1), the average radius $a = \sqrt{a_1^2 + a_2^2}$ and two definitions of the ellipticities ϵ and e. All these parameters are biased to second order in $\rho[f_0]$. Interestingly, the average radius a is biased in the elliptical case even in the absence of a PSF convolution, as a result of covariances with other parameters. Also, it is interesting to note that the rms error and bias of a_1 and a_2 have a singularity in the circular case, but the singularity cancels when they are combined to form the mean radius a. We can also verify that the scaling of equation (9) for the variance and bias of the parameters holds up to multiplicative factors of order unity.

5 CONCLUSIONS

In this paper, we have studied the effect of noise bias on MLEs for weak lensing shape parameters in the presence of additive Gaussian noise. We have derived general expressions for the covariance and bias of ML-estimated parameters of 2D galaxy images, which are given by equations (3) and (5). The bias vanishes for linear models, but is generally non-zero for models which are non-linear in the parameters and depend on the model parametrization. To illustrate the effect of the noise bias, we have calculated analytical expressions for the variance and bias for a toy model consisting of a 2D circular Gaussian galaxy, convolved with a circular Gaussian PSF, with the galaxy size as a single free parameter. We have compared these predictions with careful numerical simulations and found them to

[1] Note that in the parametrization of Paulin-Henriksson et al. (2008) the Fisher matrix is also not quite diagonal, due to covariance terms between their rotated centroid and the position angle that they have neglected.

Table 1. Statistical errors and biases of parameters for the six-parameter elliptical Gaussian model. Errors and biases are shown to leading order in ρ.

Parameter name	Symbol a	Statistical error $(\sigma[a]/a)\rho[f_0]$	Bias $(b[a]/a)\rho[f_0]^2$
		Model parameters	
Centroid	x_1^a	$\sqrt{2\left(a_1^2\cos^2\alpha + a_2^2\sin^2\alpha\right)}/x_1^a$	0
Centroid	x_2^a	$\sqrt{2\left(a_2^2\cos^2\alpha + a_1^2\sin^2\alpha\right)}/x_2^a$	0
Amplitude	f_0	1	5/2
Major axis	a_1	$\sqrt{2}$	ϵ^{-1}
Minor axis	a_2	$\sqrt{2}$	$-\epsilon^{-1}$
Position angle	α	$2\sqrt{\epsilon^{-2}-1}/\alpha$	0
		Derived parameters	
Flux	$F^0 = f_0\sqrt{a_1 a_2}$	$\sqrt{2}$	5/2
Radius mean	$a = \sqrt{a_1^2 + a_2^2}$	$\sqrt{1+\epsilon^2}$	1
Ellipticity (quadratic)	$\epsilon = \frac{a_1^2 - a_2^2}{a_1^2 + a_2^2}$	$2(1-\epsilon^2)/\epsilon$	$2(1-\epsilon^2)/\epsilon^2$
Ellipticity (linear)	$e = \frac{a_1 - a_2}{a_1 + a_2}$	$(1-e^2)/e$	$(1-e^4)/(2e^2)$

be in good agreement. We have also provided analytical results for a 2D elliptical Gaussian with six parameters.

We find that the variance and bias of the parameters are generically of the order of ρ^{-2}, where ρ is the SNR of the galaxies. For galaxies with $\rho \sim 10$, which is typical of weak lensing surveys, this implies a bias in the parameters of the order of $\rho^{-2} \sim 0.01$. This is comparable to the weak lensing shear signal $\gamma \sim 0.02$ and nearly two orders of magnitude greater than the systematic shear tolerance required for future all-sky surveys, $\delta\gamma \sim 3 \times 10^{-4}$. Although derived using the specific case of the MLE in the presence of Gaussian noise, our results are likely to be generic across a number of measurement techniques. This may contribute towards explaining why current weak lensing surveys are limited by systematics and why finding sufficiently accurate methods has been difficult.

To solve this problem, the following ways are possible.

(i) Use higher SNR galaxies. This is an obvious solution, but it is costly in practice as it leads to a sharp drop in the useful surface density of galaxies or requires longer exposure times and/or larger telescopes.

(ii) Avoid non-linearities, either by choosing linear models or using moment-based methods. This was the idea behind shapelets methods, but we note that in all cases some level of non-linearity is unavoidable as the centroid and size (of the basis functions or weight functions) are intrinsically non-linear.

(iii) Go beyond ML estimation by using, e.g., Bayesian methods or other averaging techniques. For instance, the introduction of stacking methods was a breakthrough in the GREAT08 challenge (Bridle et al. 2009).

(iv) Calibrate the bias. While order-by-order correction methods exist for the MLEs, the models used in practice to model galaxies (e.g., exponential, de Vaucouleur, Sérsic or a multicomponent combination) convolved with observed PSFs will be complex and thus will not offer analytical expressions for the bias. Instead, numerical simulations will be needed for the bias calibration. This is the approach described in the accompanying paper by K12.

ACKNOWLEDGMENTS

We thank Gary Bernstein, Julien Carron, Joël Bergé, Stéphane Paulin-Henriksson and Lisa Voigt for helpful discussions. SB acknowledges support from the Royal Society in the form of a University Research Fellowship, and both SB and BR acknowledge support from the European Research Council in the form of a Starting Grant with number 240672. Part of BR's work was done at the Jet Propulsion Laboratory, California Institute of Technology, under contract with NASA.

REFERENCES

Albrecht A. et al., 2006, Astrophys., preprint (astro-ph/0609591)
Amara A., Réfrégier A., 2007, MNRAS, 381, 1018
Bernstein G. M., 2010, MNRAS, 406, 2793
Bernstein G. M., Jarvis M., 2002, AJ, 123, 583
Bonnet H., Mellier Y., Fort B., 1994, ApJ, 427, L83
Bridle et al., 2009, AnApS, 3, 6
Bridle S., Kneib J.-P., Bardeau S., Gull S., 2002, in Natarajan P., ed., Proc. Yale Cosmology Workshop 'The Shapes of Galaxies and Their Dark Halos'. World Scientific Press, Singapore, p. 38
Cramér H., 1999, Princeton Landmarks in Mathematics and Physics: Mathematical Methods of Statistics. Princeton Univ. Press, Princeton, NJ
Fisher R. A., 1922, R. Soc. Lond. Philos. Trans. Series, 222, 309
Heymans C. et al., 2006, MNRAS, 368, 1323
Hirata C. M. et al., 2004, MNRAS, 353, 529
Hoekstra H., Jain B., 2008, Annu. Rev. Nucl. Part. Sci., 58, 99
Hosseini R., Bethge M., 2009, Technical report, Max Planck Institute for Biological Cybernetics
Kacprzak T., Zuntz J., Rowe B., Bridle S., Refregier A., Amasa A., Voight L., Hirsch M., 2012, MNRAS, arXiv:1203.5049
Kaiser N., 2000, ApJ, 537, 555
Kaiser N., Squires G., Broadhurst T., 1995, ApJ, 449, 460
Kuijken K., 1999, A&A, 352, 355
Lewis A., 2009, MNRAS, 398, 471
Massey R. et al., 2007, MNRAS, 376, 13
Melchior P., Böhnert A., Lombardi M., Bartelmann M., 2010, A&A, 510, A75
Miller L., Kitching T. D., Heymans C., Heavens A. F., van Waerbeke L., 2007, MNRAS, 382, 315
Paulin-Henriksson S., Amara A., Voigt L., Refregier A., Bridle S. L., 2008, A&A, 484, 67
Paulin-Henriksson S., Refregier A., Amara A., 2009, A&A, 500, 647
Peacock J., Schneider P., 2006, The Messenger, 125, 48
Rao C., 1973, Wiley Series in Probability and Mathematical Statistics: Linear Statistical Inference and Its Applications. Wiley, New York

Refregier A., 2003, ARA&A, 41, 645
Refregier A., Bacon D., 2003, MNRAS, 338, 48
Rowe B., 2010, MNRAS, 404, 350
Tyson J. A., Wenk R. A., Valdes F., 1990, ApJ, 349, L1
Voigt L. M., Bridle S. L., 2010, MNRAS, 404, 458

APPENDIX A: BIAS FOR A GENERAL MLE

In this appendix, we provide the derivation of the main results for the variance and bias of a general MLE of parameters given in Section 2 for additive, uncorrelated Gaussian noise. For the model describe in Section 2, the likelihood is

$$L \propto \mathrm{e}^{-\chi^2/2}, \tag{A1}$$

where

$$\chi^2(\boldsymbol{a}) = \sum_p \sigma_\mathrm{n}^{-2} \left[f(\boldsymbol{x}_p; \boldsymbol{a}^\mathrm{t}) + n(\boldsymbol{x}_p) - f(\boldsymbol{x}_p; \boldsymbol{a}) \right]^2 . \tag{A2}$$

The MLE $\hat{\boldsymbol{a}}$ is then defined as the value of the parameters $\boldsymbol{a}$ which maximizes the likelihood L or, equivalently, which minimizes χ^2, i.e. for which

$$\left. \frac{\partial \chi^2}{\partial \boldsymbol{a}} \right|_{\hat{\boldsymbol{a}}} = 0. \tag{A3}$$

To proceed, we expand this expression in terms of the inverse of the SNR, $\rho \sim f/n$, of the object. This can be conveniently done by rewriting $n(\boldsymbol{x}_p) \rightarrow \alpha n(\boldsymbol{x}_p)$ and $\hat{\boldsymbol{a}} = \boldsymbol{a}^\mathrm{t} + \alpha \delta \boldsymbol{a}^{(1)} + \alpha^2 \delta \boldsymbol{a}^{(2)} + \cdots$, where α is a dimensionless order parameter which scales as $\alpha \sim \rho^{-1}$. We then Taylor expand $f(x, a)$ about a^t, collect like powers of α in equation (A3) and set $\alpha = 1$. The terms of order α yield

$$\delta a_i^{(1)} = (F^{-1})_{ij} \sum_p \sigma_\mathrm{n}^{-2} n(\boldsymbol{x}_p) \frac{\partial f(\boldsymbol{x}_p; \boldsymbol{a})}{\partial a_j}, \tag{A4}$$

where the fisher matrix F_{ij} was defined in equation (4). Taking the average of this expression and using the fact that the noise is unbiased, i.e. $\langle n(\boldsymbol{x}_p) \rangle = 0$, we see that the estimator is unbiased to this order. Taking the average of the product $\langle \delta a_i^{(1)} \delta a_j^{(1)} \rangle$ and using the fact that the noise is uncorrelated, i.e. $\langle n(\boldsymbol{x}_p) n(\boldsymbol{x}_{p'}) \rangle = \delta_{p,p'} \sigma_\mathrm{n}^2$, we obtain the expression for the covariance of the parameters to leading order given in equation (3).

The terms of order α^2 yield

$$\delta a_i^{(2)} = -\frac{1}{2} (F^{-1})_{ij} (F^{-1})_{kl} B_{jkl}, \tag{A5}$$

and thus gives equation (5) for the bias to leading order, where the bias tensor was defined in equation (6).

These results can also be derived from the general expressions of the Fisher matrix

$$F_{ij} = \left\langle -\frac{\partial^2 \ln L}{\partial a_i \partial a_j} \right\rangle \tag{A6}$$

and for the bias tensor for the MLE

$$B_{ijk} = \left\langle -\frac{1}{2} \frac{\partial^3 \ln L}{\partial a_i \partial a_j \partial a_k} + \frac{\partial \ln L}{\partial a_j} \frac{\partial^2 \ln L}{\partial a_i \partial a_k} \right\rangle . \tag{A7}$$

In the limit of small pixels, the sum over pixels in the expressions above can be approximated by a continuous integral

$$\sum_p \simeq \int \frac{\mathrm{d}^2 x}{h^2}, \quad \text{as } h \rightarrow 0, \tag{A8}$$

where h is the pixel size.

APPENDIX B: RESULTS FOR THE ELLIPTICAL GAUSSIAN MODEL

In this appendix, we provide results for the elliptical Gaussian model defined in equation (18) as a function of the six parameters listed in equation (21) in the presence of additive, uncorrelated Gaussian noise as defined in equation (1).

With this parametrization, the flux or zeroth-order moment of the Gaussian is given by

$$F^{(0)} = \int \mathrm{d}^2 x f(\boldsymbol{x}; \boldsymbol{a}) = f_0 \sqrt{a_1 a_2}. \tag{B1}$$

The centroid or first-order moments are given by

$$\frac{F_i^{(1)}}{F^{(0)}} = \frac{1}{F^{(0)}} \int \mathrm{d}^2 x x_i f(\boldsymbol{x}; \boldsymbol{a}) = x_i^a, \tag{B2}$$

and the quadrupole moment matrix, containing the second-order moments, is given by

$$\frac{F_{ij}^{(2)}}{F^{(0)}} = \frac{1}{F^{(0)}} \int \mathrm{d}^2 x x_i x_j f(\boldsymbol{x}; \boldsymbol{a}) = A_{ij}. \tag{B3}$$

For this model, in the continuum limit (equation A8), the Fisher matrix F_{ij} (equation 4) can be derived analytically by rotating into a coordinate system with axes parallel to the major and minor axes of the galaxy (using the rotation matrix in equation 20) before performing the integrals over the surface of the galaxy. Note that this procedure still leaves the position angle α as a free parameter. The covariance matrix of the parameters is then obtained by inverting the Fisher matrix (equation 3) which yields

$$\mathrm{cov}[\hat{a}_i, \hat{a}_j] = \begin{pmatrix} 2A_{11} & 2A_{12} & 0 & 0 & 0 & 0 \\ 2A_{12} & 2A_{22} & 0 & 0 & 0 & 0 \\ 0 & 0 & {f_0}^2 & 0 & 0 & 0 \\ 0 & 0 & 0 & 2a_1^2 & 0 & 0 \\ 0 & 0 & 0 & 0 & 2a_2^2 & 0 \\ 0 & 0 & 0 & 0 & 0 & \frac{4a_1^2 a_2^2}{(a_1^2 - a_2^2)^2} \end{pmatrix} \times \rho[f_0]^{-2} + O(\rho^{-3}), \tag{B4}$$

where A_{ij} are the components of the quadrupole moment matrix $\mathbf{A}$ defined in equation (19), and $\rho[f_0]$ is the SNR of the amplitude f_0 given in equation (22). While the Fisher matrix is conveniently nearly diagonal to this order, higher order terms contribute to off-diagonal elements correlating, for instance, the centroid with the shape parameters.

The bias in the parameters can be derived using equation (5) which yields

$$\frac{b[a_i]}{a_i} = \left(0, 0, \frac{5}{2}, \epsilon^{-1}, -\epsilon^{-1}, 0\right) \rho[f_0]^{-2} + O(\rho^{-3}), \tag{B5}$$

where the quadratic ellipticity ϵ is defined in Table 1.

The resulting rms errors and biases for the model parameters are summarized in the upper part of Table 1.

This paper has been typeset from a TEX/LATEX file prepared by the author.